

Optimizing the axial distance of the nozzle to the engine shell to cool the maximum fluid flow

Sajad Rastad^a, Seyed AmirAbbas Oloomi^{a,*}, Seyed AliAgha Mirjalily^a, Abolfazl Zare-Shahabadi^b

^aDepartment of Mechanical Engineering, Yazd Branch, Islamic Azad University, Yazd, Iran

^bDepartment of Mechanical Engineering, Technical and Vocational University (TVU), Tehran, Iran

(Communicated by Madjid Eshaghi Gordji)

Abstract

The purpose of this paper is to obtain the optimal axial distance from the nozzle to the motor shell for suction of the maximum flow rate of the cooling fluid. Given that there is no laboratory data to evaluate numerical analysis, an attempt was made to validate the numerical coefficient of the NACA0012 blade lift by numerical method to validate the numerical method and compare it with its existing laboratory results. As you can see from the results, the distance between the nozzle and the motor has a very small effect on the cooling flow. In fact, this shows that with the changes in axial distance in the mentioned range (between 0 and 2.5 cm), the amount of suction caused by the hot jet of the hot nozzle output of the nozzle has a very small effect on the cooling flow. To check the suction rate of the nozzle output jet on the cooling flow rate, the problem for different discharge nozzles is numerically analyzed to see how much the effect of the nozzle output fluid on the cooling fluid discharge flow is. The coolant flow of the Flow rate engine nozzle does not change much. This factor indicates that the flow rate of the engine coolant flow is mostly due to the pressure of the coolant itself and does not depend on the suction jet of the nozzle output. In this section, the effect of increasing the length of the engine shell on the cooling rate of the engine cooling is discussed. In this analysis, the shell length was increased by 6.5 cm. The increase in shell length is done with a constant diameter. As the shell length increased, the cooling flow rate increased significantly. As the shell length increases, the cooling flow rate increases by about 52% at the relative inlet pressure of 15,000 Pascals.

Keywords: nozzle, engine shell, Flow rate suction, cooling.

2010 MSC: 82Dxx

*Corresponding author

Email addresses: Rastadsajad@yahoo.com (Sajad Rastad), Amiroloomi@iauyazd.ac.ir (Seyed AmirAbbas Oloomi), Saa_mirjalily@iauyazd.ac.ir (Seyed AliAgha Mirjalily), Abzare@tvu.ac.ir (Abolfazl Zare-Shahabadi)

Received: October 2021 *Accepted:* December 2021

1. Introduction

In this paper, the goal is to obtain the optimal axial distance from the nozzle to the motor shell in order to absorb the maximum flow rate of the cooling fluid. In fact, these analyzes will try to find the best distance. In the final part of this section, the effect of shell length on the cooling flow rate is examined and finally it is seen that with increasing the length of the cooling flow rate, the cooling rate increases by about 50%. Due to the fact that there is no laboratory data to evaluate numerical analysis, for this reason, an attempt was made to validate the numerical method, obtain the NACA0012 vanity lift coefficient by numerical method and compare it with its existing laboratory results. A comparison between the numerical and laboratory results for the NACA0012 blade showed the accuracy of the numerical method used. Haas et al. [13] investigated the effect of injection density on the cooling effect of the blade layer of a gas turbine in the open state with low turbulence. They found that at 0.5 injections, a higher density created better layer cooling effects. Laogowski and Gol [16] conducted an empirical-numerical study taking into account the secondary flow and the layered cooling effects in the development of secondary flows. In this study, they used a series of holes in the escape edge of the fixed turbine blade and, with a numerical simulation, solved the Navirastox equations in three dimensions and compared the experimental and numerical solution functions.

For the internal cooling of the blades, the displacement cooling work is also used, and a lot of research has been done in this regard. For example, Alhajari et al. [4] have conducted a numerical study of flow and heat analysis in cooling ducts inside turbine blades. However, this study was performed on a U-shaped channel with semicircular turbulators. Roy et al. [24] have conducted research on the design and optimization of the cooling system using the genetic algorithm. Ghobadi et al. [12] also investigated the effect of stimulating the border layer in a pre-cooling cooling channel and its effect on the pre-cooling work.

Little research has been done on the use of genetic algorithms in boundary layer excitation studies. And Collins et al. [10] investigated the dome-shaped protrusions on the screen and showed that the heat transfer coefficient increases in some places and decreases in others. Bahavanani and Bergels [7] used the laboratory method to investigate the effect of large protrusions on the surface. Choi et al. [8] conducted an experimental study on a concave grooved jet colliding with a concave semicircular surface at different distances and with different Reynolds numbers, and reported the effect of this collision on changes in wall number and hydrodynamic characteristics.

Liu and Feng [18] performed a numerical simulation to investigate the amount of cooling caused by the jet hitting the front edge of the gas turbine blade. The results showed that the average Nasturtium number at the edge of the blade increased with increasing Mach Jet number as well as decreasing the nozzle output distance to the wall. Also, a relationship for calculating the average Naslett number was presented as a function of the considered parameters. Also, by examining the number of Naslett in the direction of the wall and the longitudinal direction, it was observed that the average Naslett number increases with increasing the Mach number and decreasing the jet distance to the wall. Tehrani and Mahmoudi [6] examined the effect of injection angle and severity of turbulence in the flow and temperature field in the method of cooling single-hole layers in three dimensions using the finite element method with cubic elements. In this analysis, the best angle The injection was reported to be 35 best C and the best inhalation ratio was 0.5. C, according to experimental results.

A numerical modeling was performed by Liu et al. [20] Using a combination of collision cooling technique and cooling front edge layer of gas turbine blades. In this study, it was shown that the $k - \omega$ SST model is the most accurate model for predicting the flow field and heat transfer compared to the available experimental results. In addition, in this study, a row of jets with three rows of ducts

was considered for layer cooling and an increase in heat transfer coefficient on the edge of the blade was reported by increasing the flow rate and changes in the angle of the coolant passage.

Other research has included the research of Sun et al. [25], in which dual methods for numerical study of the cooling film of turbine blades are also mentioned. Also, Horlock et al. [14] The cooling air flow (cooling of the external film and cooling of the internal convection) has affected the performance of the gas turbine. The results showed that reducing the pressure of the inlet still to the first rotor and the pressure drop due to mixing of the cooling air with the main flow has the most important effect on the cooling of the turbine blade. In 2002, Amell and Cadavid [5] studied the effect of relative humidity on the performance of the cooling system in atmospheric air. They concluded that at high relative humidity, heat transfer is about twice as low as relative humidity. In 2002-2004, Turbidoni et al. [26] proposed an analytical method for calculating the required cooling flow in the first stage of high-pressure gas turbine with gas inlet temperature and cooling fluid. In 2009, Clinton and colleagues [9] examined the optimization of cooling cycles in the turbine blade. The results showed that in moistened air turbine blades, the need for coolant was reduced but increased compressor operation. In 2011, Kim et al. [15] examined the turbine blade with ten internal drilling paths from the point of view of heat transfer and the stresses created. The results of their research have shown that the highest heat transfer coefficient is related to the eighth hole from the edge of the attack. In 2015, Abdullah et al. [3] investigated the numerical cooling simulation of turbine blades through JET collisions. In this simulation, the numerical model was simulated by considering uniform uniform shear applications on a curved surface exposed to a flow jet. A channel was installed under the blade for cooling.

In 2016, Moskalenko et al. [23] Estimated the cooling rate of gas turbine blades. This paper examines the results of the thermal stress assessment of gas turbine elements and also examines the power of turbine blades and cooling efficiency. Here, the calculations are based on a numerical simulation based on the finite element. The average temperature of the heat transfer coefficient, from the average cooling to the cooling channels of the walls, is used by Ensis Fluent software.

In 2015, Cheng et al. [11] examined the effects of jet nozzle geometry on the flow and heat transfer of Vertex cooling of turbine gas blades. In this paper, a three-dimensional Reynolds model and the NeuerStokes equations are used to show the effects of nozzle geometry on flow and temperature behavior, and the Vertex cooling of gas turbine blades. A comparison has also been made between the calculations of the turbulent model and the laboratory results. The results show that the k model is used for simulation.

In 2016, Xu et al. [17] investigated the turbulent flow on cooling of turbine blades. In this study, a combined effect of turbocharging current intensity and rotation ratio on cooling and performance of turbine blades. Sensitive color injection is given.

In 2016, Mazaheri et al. [22] investigated the optimization of pre-turbine cooling using conjugate heat transfer technique. In this analysis, an optimized sample of the shape of the turbine blade and the location of the cooling channels of a turbine blade using the conjugate heat technique are discussed.

A finite volume method is used to solve the equations [1, 2]. The turbulent intensity is 5% and the mass imbalance is less than 0.001%. Aerodynamic static stability and generation of sufficient thrust are the major problems of a hypersonic ram jet-propelled vehicle [27, 19], whereby the nozzle and external base flow interaction play a large role.

2. Modeling

After extracting the points from the existing solidwork maps, these points enter the Gambit software. In this software, geometry is reproduced and grided. Geometry production is the best time among numerical analysis steps. The size of the grid and its type (organized, disorganized, or combined) have a great impact on the resolution time, convergence rate, or even the non-convergence and accuracy of the responses. To produce a grid, the user must have the right ratio of physics to be able to create a suitable grid in places where the solution field has more gradients (pressure, temperature and velocity). In addition to griding in this software, the border conditions are set without giving a value in it.

The file generated by Gambit software enters Fluent software to solve current equations (Navier-Stokes equations). In this software, the values of the boundary conditions are determined. One of the most important settings in this software is to determine whether the current is quiet or turbulent. Given the Reynolds number, the flow is quite turbulent. So the flow must be modeled in a chaotic voice. Determining the turbulent model is one of the most important steps in numerical solution, which explains how to choose the turbulence model in the following sections. This paper uses the k-ε SST model, which is based on averaging models. In fact, it is a combination of the K-Omega Standard and K-Epsilon turbocharged models. In this turbocharged model, near the wall, the K-omega model, which is a low Reynolds model, is used, and in the cross-border areas, the k-epsilon model, which is a high Reynolds model, is used. In this way, the positive feature of the two turbocharged models will be used. According to NASA, this model is the most efficient turbocharged model known for industrial issues. Also, this model has the best estimate of current separation compared to other models. In the present model, due to the high flow rate and curvature of the liner wall, it is predicted that the separation phenomenon will be seen in the flow. Also, due to the use of the K-Epsilon model in the dominant part of the range, it has a good convergence rate and its sensitivity to input and remote clutter conditions is low. Finally, due to the ability to simulate the entire solution range to the vicinity of the wall, it has the ability to identify and indicate the occurrence of separation around objects. Another advantage of the SST is its lower sensitivity to the adjacent height of the wall (Y^+) in the range below 100, while in models such as the K-Epsilon with Y^+ change, local values on the wall such as strain rate and subsequent stress rate. The cut undergoes more drastic changes. Below is a comparison of the sensitivity of these two models to the amount of Y^+ in the vicinity of the indicated wall. Finally, considering the main sensitivity of the article on turbulent elements on the volume and amount of separation, the decision to choose the SST model as the current simulation confusion model was made. The SST model is a two-equation model. The first equation is the turbulent energy transfer and the second equation is the vortex frequency.

The governing equations used are as follows:

Mass conservation equation:

$$\frac{\partial p}{\partial t} + \frac{\partial}{\partial x}(\rho v_x) + \frac{\partial}{\partial r}(\rho v_r) + \frac{\rho v_r}{r} = 0 \quad (2.1)$$

Momentum conservation equation:

$$\frac{\partial}{\partial t}(\rho v_x) + \frac{1}{r} \frac{\partial}{\partial x}(r \rho v_x v_x) + \frac{1}{r} \frac{\partial}{\partial r}(r \rho v_r v_x) = -\frac{\partial p}{\partial x} + \frac{1}{r} \frac{\partial}{\partial x} [r \mu (2 \frac{\partial v_x}{\partial x} - \frac{2}{3} (\nabla \cdot \mathbf{v}))] + \frac{1}{r} \frac{\partial}{\partial r} [r \mu (\frac{\partial v_x}{\partial r} + \frac{\partial v_r}{\partial x})] \quad (2.2)$$

And

$$\frac{\partial}{\partial t}(\rho v_r) + \frac{1}{r} \frac{\partial}{\partial x}(r \rho v_x v_r) + \frac{1}{r} \frac{\partial}{\partial r}(r \rho v_r v_r) = -\frac{\partial p}{\partial r} + \frac{1}{r} \frac{\partial}{\partial x} [r \mu (\frac{\partial v_r}{\partial x} + \frac{\partial v_x}{\partial r})] + \frac{1}{r} \frac{\partial}{\partial r} [r \mu (2 \frac{\partial v_r}{\partial r} - \frac{2}{3} (\nabla \cdot \mathbf{v}))]$$

Table 1: The flow rate of cooling elements

Cooling fluid flow rate	Number of grid
0.34416248	48100
0.34479920	311494

$$-2\mu \frac{v_r}{r^2} + \frac{2\mu}{3r} (\nabla \cdot \mathbf{v}) \tag{2.3}$$

where:

$$\nabla \cdot \mathbf{v} = \frac{\partial v_x}{\partial x} + \frac{\partial v_r}{\partial r} + \frac{v_r}{r} \tag{2.4}$$

Energy equation:

$$\frac{\partial}{\partial t}(\rho E) + \frac{\partial}{\partial x_j} [u_i(\rho E + p)] = \frac{\partial}{\partial x_j} [(k_T + \frac{C_p \mu_t}{Pr_t}) \frac{\partial T}{\partial x_j} + u_j(\tau_{ij})_{eff}] \tag{2.5}$$

The shear stress transport (SST) $k - \omega$ model was used [21], in which the $k - \omega$ model was used in the near-wall region and the $k - \epsilon$ model was applied in the far-field which was not affected by the free stream. Menter’s SST $k - \omega$ model provides a reasonable prediction of nozzle flow separation, and different shocks occur due to overexpansion and under expansion. Transport equations for the SST $k - \omega$ model are given by:

$$\frac{\partial}{\partial t}(\rho k) + \frac{\partial}{\partial x_j}(\rho k u_i) = \frac{\partial}{\partial x_j}(\Gamma_k \frac{\partial k}{\partial x_j}) + G_k + Y_k \tag{2.6}$$

and [25, 26]:

$$\frac{\partial}{\partial t}(\rho \omega) + \frac{\partial}{\partial x_j}(\rho \omega u_i) = \frac{\partial}{\partial x_j}(\Gamma_\omega \frac{\partial \omega}{\partial x_j}) + G_\omega - Y_\omega + D_\omega \tag{2.7}$$

Boundary conditions:

1. In all nozzle walls, it is assumed that the surface speed of the walls is zero.
2. The boundary condition on the surface of the hemisphere (the environment around the nozzle) is assumed at the input of the pressure inlet and at the output of the pressure outlet.
3. Mass Flow Inlet border condition is used in the nozzle output.
4. Pressure Inlet is used for air inlet holes.
5. In this issue, for the two-dimensional analysis, the boundary condition of axial symmetry has been used.

Finding the optimal grid for which the answer to the problem is independent of the grid and at the same time the production grid is the largest grid in accordance with the above property. It is quite experimental and time consuming. Usually, to find such a grid, we draw a graph of the changes in the answers according to the number of nodes in the grid, and at each stage we increase the number of nodes, and finally we repeat this until the changes reach an acceptable level. The selected parameter for investigating the independence of the solution from the Flow rate mass grid is the coolant fluid (fluid passing between the nozzle and the shell). Initially, the number of elements was about 48,100. After the grid was shredded near the walls, the number of elements produced was finally determined by Gambit software 311494.

Adoption Grid is used in Fluent software to break the network. Due to the fact that the k-w sst clutter model was used to simulate the turbulent flow, the network was shrunk to a point where the contour + y near the walls was less than one.

Table 2: The rate of cooling flow rate according to the pressure of the cooling fluid and the axial distance of the motor nozzle to the shell

Axial distance from the shell to the engine nozzle	P = 10000	P = 15000	P = 20000	P = 25000	P = 30000
0	0.21673637	0.34742791	0.44596988	0.52841445	0.60070461
0.5		0.34638923	0.44515337	0.52774101	0.60013179
1.5	0.21271856	0.34509491	0.44422132	0.52699145	0.59951428
2.5	0.21452137	0.34416248	0.44178671	0.52359997	0.59543942

3. Results from simulation

The contour of the Mach number around the blade is perfectly symmetrical, and there is no reverse flow at any point in the solution area. Also, due to the symmetry of the blade, the velocity vectors at the end of the blade are completely parallel, indicating that the current does not deviate. Comparison of numerical and experimental results shows the accuracy of the numerical method used. The maximum error rate at the angle of attack is close to the stall and its value is about 4%. As can be seen, there is a good match between numerical and experimental results, which is an indication of the accuracy of the numerical method used.

3.1. Obtaining the axial distance of the motor nozzle to the shell in order to achieve the maximum cooling flow rate of the motor

In this section, with the changes in the axial distance of the nozzle to the shell, the most optimal distance is obtained to achieve the highest engine cooling flow rate. The axial distance between the shell and the nozzle is chosen between 0 and 2.5 cm. Analysis is performed for intervals of 0 and 5.5, 1.0 and 2.5. Since there is no laboratory data for engine coolant pressure, the value of the pressure gauge is 1.1 to 1.3 times and in numbers 1.1, 1.15, 1.2, 1.25, 1.3 times to ensure that the optimal distance is selected. Table 2 shows the rate of cooling flow rate according to the pressure of the cooling fluid and the axial distance of the motor nozzle to the shell.

As can be seen from the results of Table 2, the optimal distance between 0 and 0.5 must be selected. But as you can see, the distance between the nozzle and the engine has a very small effect on the cooling flow rate. In fact, this shows that with the changes in axial distance in the mentioned range (between 0 and 2.5 cm), the amount of suction caused by the hot jet output jet of the nozzle output has a very small effect on the cooling flow rate. To check the suction rate of the nozzle output jet on the cooling flow rate, the problem for the different nozzle output flow rates is numerically analyzed to see what the effect of the nozzle output fluid is on the coolant flow rate. In fact, an attempt is being made to answer the question of whether the rate of the coolant flow rate is due to the fluid pressure itself or to the rate of suction from the nozzle output jet. In fact, with this analysis, a small amount of suction from the nozzle output jet can be obtained at the coolant flow rate. Table 3 shows the effect of nozzle output flow rate on the rate of mass flow rate of engine coolant. As can be seen, with the change in the flow rate of the engine nozzle, the coolant flow rate does not change much. This factor indicates that the flow rate of the engine coolant flow is mostly due to the pressure of the coolant itself and does not depend on the suction jet of the nozzle output.

3.2. Investigating the effect of increasing engine shell length on engine cooling rate

In this analysis, the shell length was increased by 6.5 cm. The increase in shell length is done with a constant diameter. When the fluid exits the nozzle, the flow nozzle expands a few centimeters,

Table 3: The effect of nozzle output flow rate on mass flow rate of engine coolant fluid

Cooling fluid flow rate	Nozzle output current rate
0.34742791	7
0.34450494	6
0.34017925	5
0.34012727	4

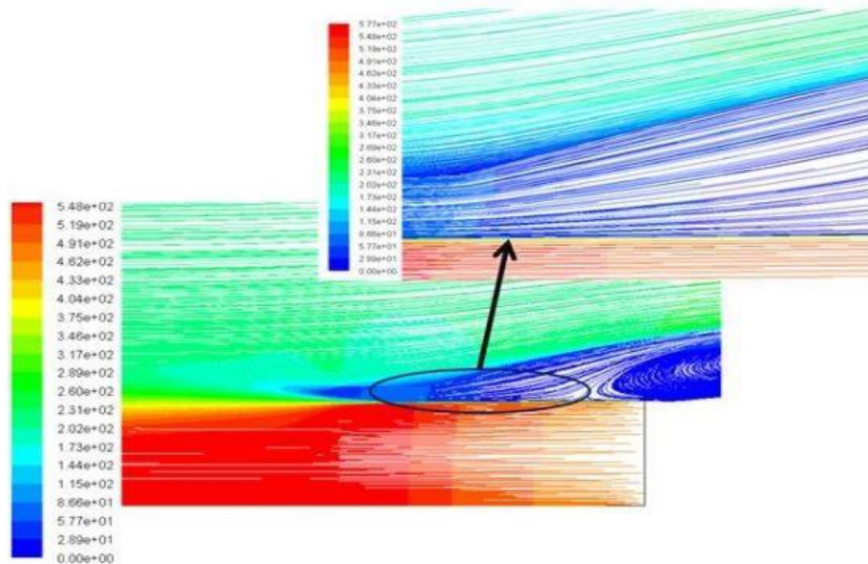


Figure 1: Current lines in the nozzle area of the motor with increasing shell length

and this expansion of the fluid flow causes the surrounding flow to be sucked. One of the factors that reduces the rate of cooling flow is the fluid flow around the bird (Far Field). The air flow around the nozzle at the outlet due to its high pressure tends to go into the gap between the shell and the nozzle (the entry point of the coolant). This reduces the flow rate of the coolant (the cause of the vortex at the nozzle output is the mixing of the fluid around the bird and the coolant. Increasing the shell length causes the remote current around the Far Field nozzle output) to fail.

The output of the current is disconnected. As the shell length increased, the cooling flow rate increased significantly. As the shell length increases, the cooling flow rate increases by about 52% at the relative inlet pressure of 15,000 Pascals. In this report, the effect of increasing shell length (shell length increased to a constant value) is simulated by changing the length. The following is the rate of cooling flow rate for different nozzle lengths in Table 4.

One of the parameters that affects the cooling effect of the film is the thermal flux ratio. Thermal flux ratio is used as a physical justification for choosing the blowing ratio. The ratio of thermal flux is as follows:

$$I = \frac{\rho_j V_j^2 j}{\rho_\infty V_\infty^2}$$

Where I is the ratio of thermal flux. The temperature and velocity of the mainstream are K 288 and 15 m/s, respectively. The injected cooling air temperature is 250, 328, 340 and 350 K, respectively. The values of thermal flux ratio in this table 5 are given for this blowing ratio.

The effect of network size on numerical results was studied in order to obtain a network size that

Table 4: The rate of cooling flow rate according to the cooling fluid pressure and axial distance of the motor nozzle to the shell (shell length increased by 6.5 cm)

Axial distance from the shell to the engine nozzle	P = 10000	P = 15000	P = 20000	P = 25000	P = 30000
0	0.45556474	0.52456781	0.58656976	0.64376122	0.69738882
0.5	0.44554323	0.52102496	0.58265787	0.64070866	0.69460017
1.5	0.44554323	0.51630001	0.57970082	0.63756418	0.69217069
2.5	0.44420989	0.51447087	0.57811508	0.63665765	0.69117206

Table 5: Values of thermal flux ratio

$T_j(K)$	$\rho_j(kg/m^3)$	ρ_j/ρ_∞	$U_j(m/s)$	U_j/U_∞	M	I
250	1.417332	1.163	6.590	0.440	0.6	0.229
330	1.087541	0.991		0.564	0.6	0.289
340	1.039662	0.850	8.87	0.591	0.6	0.300
355	1.009114	0.830		0.619	0.6	0.315
250	1.413028	1.157	9.768	0.652	0.80	0.482
335	1.080995	0.880	12.86	0.856	0.80	0.645
350	1.039442	0.850	13.29	0.890	0.80	0.662
355	1.007785	0.824	13.680	0.9120	0.80	0.690

does not require accurate solutions and a large amount of memory and computer time. The number of network cells on the measurement surface increased until constant solutions were obtained. The temperature change at the measurement level was compared in each sample and the desired number of networks for geometry was selected. When the number of grids increases from 250,000 to 240,000, the temperature change is 0.1196% and 0.1509%, respectively, along the E level in the main flow direction and along the B level in the lateral direction.

The three-dimensional temperature field was calculated for different levels of curvature and blowing ratio. Then, the coolant efficiency of the adiabatic film of temperature was calculated using the following equation:

$$\eta = \frac{T_{adiabatic} - T_\infty}{T_j - T_\infty}$$

Where is the film’s cooling effects are, is the adiabatic wall temperature, is the main flow $\eta T_{adiabatic} T_\infty$ temperature, and is the liquid temperature injected. The results obtained for the hole in the middle for T_j all levels are given below. The following results were found for the effects of temperature ratio

Table 6: Effect of network size from 250,000 to 240,000 increased in numerical results of 0.75 blowing ratio

Surface	Change of temperature			
	Mainstream direction		Lateral direction	
	Min (%)	Max (%)	Min (%)	Max (%)
A	0.0159	0.0405	-0.0460	0.0151
B	-0.0047	0.0376	-0.0660	0.1507
C	0.0008	0.0504	0.0002	0.0618
D	0.0012	0.0510	0.0010	0.0498
E	0.0190	0.1200	-0.0528	0.01199

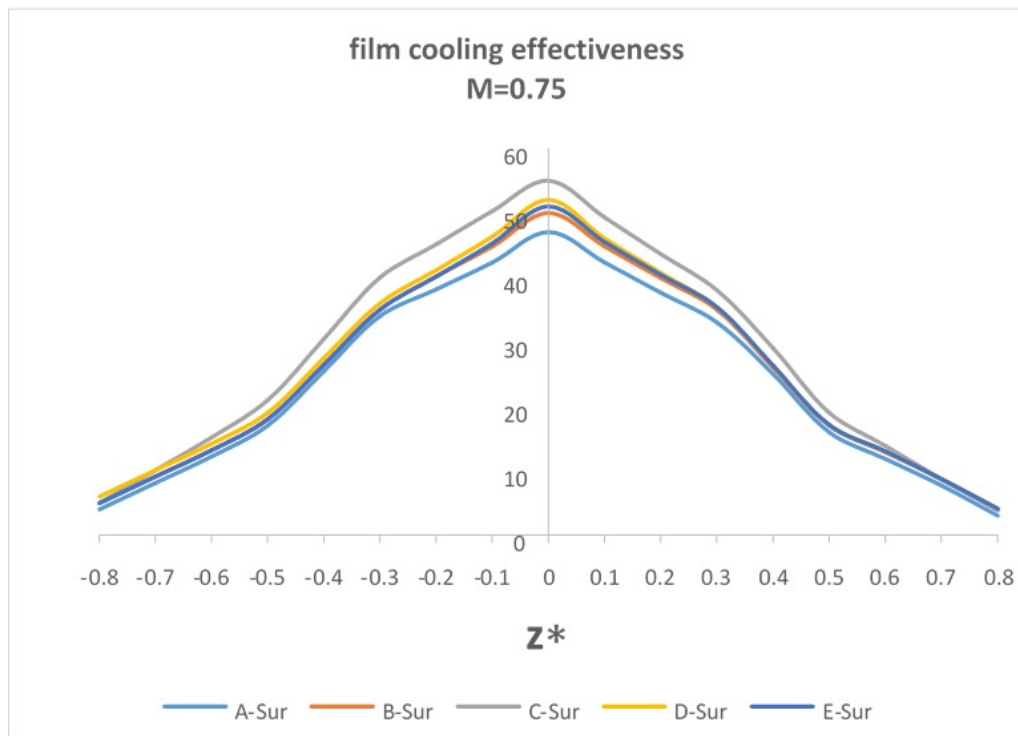


Figure 2: Comparison of levels in the blowing ratio of 0.75 in the lateral direction. Cooling film sizes were obtained in the lateral direction at $x^* = 1$. The lateral direction is indicated by z^* , where $z^* = z/L$ is a certain length (7.25 L = mm is taken for this study). Although the cooling effect of the film decreases from 0.5 to 1.0 relative to blowing, the tail ratio increases from 1.0 to 2.0 in the lateral direction. Level C has the best cooling effect of the film in blowing 0.75. Comparison of blowing ratios and film cooling levels.

and surface curvature on the cooling effects of the film in the main flow and in the lateral direction.

3.3. Efficiency is the best C geometry and the best blow ratio is 0.75 on the side

In figure 3, level C has highest value of cooling efficiency at a blowing ratio of 0.75. The cooling effect of the film is 68% for the C level at $1x^* =$ at a blowing ratio of 0.75, while $x^* = x/L$ is the characteristic length (7.25 L = mm is taken for this study). The cooling effect of the film is D 67% and E 66% in similar conditions. Level C has the best cooling effect of the film at $1x^* =$ in all blowing ratios.

4. Conclusion

The purpose of this analysis was to obtain the optimal axial distance from the nozzle to the motor shell to suck the maximum coolant flow rate. In fact, these analyzes tried to find the most optimal distance. Since there is no laboratory data to evaluate numerical analysis, an attempt was made to validate the numerical coefficient of the NACA0012 blade lift by numerical method and to compare it with its existing laboratory results. A comparison between the numerical and laboratory results for the NACA0012 blade showed the accuracy of the numerical method used. The axial distance between the shell and the nozzle was selected between 0 and 2.5 cm. The analysis was performed for intervals of 0, 0.5, 1.0 and 2.5. Given that there were no laboratory data for engine coolant fluid pressure, the amount of fluid cooling pressure was between 1.1 to 1.3 times and 1.1, 1.5, 1.2, 1.25, 1.3 times to ensure the optimal distance. As can be seen from the results of Table 2, the optimal

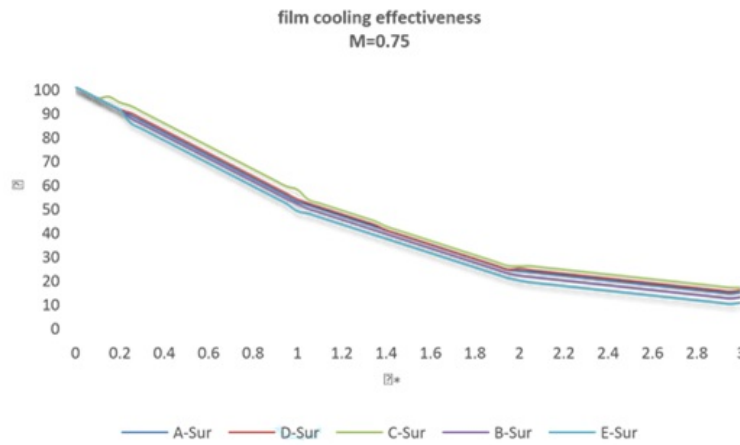


Figure 3: Cooling efficiency at a blowing ratio of 0.75

distance between 0.5 must be selected. However, as can be seen from the results of Table (3), the distance between the nozzle and the motor has a very small effect on the cooling flow rate. In fact, this shows that with the changes in axial distance in the mentioned range (between 0 and 2.5 cm), the amount of suction caused by the hot jet output jet of the nozzle output has a very small effect on the cooling flow rate. To check the suction rate of the nozzle output jet on the cooling flow rate, the problem for the different nozzle output flow rates is numerically analyzed to see what the effect of the nozzle output fluid is on the coolant flow rate.

As can be seen from the results of Table 3, by changing the flow rate of the engine nozzle, the coolant flow rate does not change much. This factor indicates that the flow rate of the engine coolant flow is mostly due to the pressure of the coolant itself and does not depend on the suction jet of the nozzle output. In this section, the effect of increasing the length of the engine shell on the engine cooling rate is discussed. In this analysis, the shell length was increased by 6.5 cm. The increase in shell length is done with a constant diameter. As the shell length increased, the cooling flow rate increased significantly. As the shell length increases, the cooling flow rate increases by about 52% at the relative inlet pressure of 15,000 Pascals.

References

- [1] M. Ahmadi and F.A. Khosravi, *CFD simulation of non-Newtonian two-phase fluid flow through a channel with a cavity*, Thermal Sci. 24(2B) (2020) 1045–1054.
- [2] M. Ahmadi, S.A.A. Mirjalily and S.A.A. Oloomi, *RANS $K - \omega$ simulation of 2d turbulent natural convection in an enclosure with heating sources*, IIUM Engin. J. 20(1) (2019) 229–244.
- [3] A.R. AlAli and I. Janajreh, *Numerical simulation of turbine blade cooling via jet impingement*, Energy Procedia 75 (2015) 3220–3229.
- [4] M. Alhajeri and H. Alhajeri, *Heat and fluid flow analysis in gas turbine blade cooling passages with semicircular turbulators*, Int. J. Phys. 4 (2009) 835–845.
- [5] A.A. Amell and F.J. Cadavid, *Influence of the relative humidity on the air cooling thermal load in gas turbine power plant*, Appl. Thermal Eng. 22(13) (2002) 1533–1529.
- [6] F. Bazdidi-Tehrani and A. Mahmoodi, *Investigation of the effect of turbulence intensity and injection angle on the flow and temperature field in the single hole film cooling technique*, Int. J. Eng. Sci. 4(12) (2002) 25–38.
- [7] S.H. Bhavnani and A.E. Bergles, *Interferometric Study of Laminar Natural Convection from An Isothermal Vertical Plate with Transverse Roughness Elements*, PHD Dissertation, Iowa State University, Iowa, 1987.
- [8] M. Choi, H.S. Yoo, G. Yang, J.S. Lee and D.K. Sohn, *Measurements of impinging jet flow and heat transfer on a semi-circular concave surface*, Int. J. Heat Mass Transfer 43(10) (2000) 1822–1811.

- [9] J. Cleeton, R. Kavanagh and G. Parks, *Blade cooling optimisation in humid-air and steam-injected gas turbines*, Appl. Thermal Eng. 29(16) (2009) 3283–3274.
- [10] M. Colins, S.J. Harrison, D. Naylor and P.H. Oosthuizen, *Heat transfer from an isothermal vertical surface with adjacent heated horizontal louvers: Numerical analysis*, J. Heat Transfer 124 (2002) 1072–1077.
- [11] C. Du, L. Li, X. Wu and Z. Feng, *Effect of jet nozzle geometry on flow and heat transfer performance of vortex cooling for gas turbine blade leading edge*, Appl. Thermal Eng. 48(7) (2015).
- [12] A. Ghobadi, M. Javadi and B. Rahimi, *Cooling turbine blades using exciting boundary layer*, World Academy Sci. Technol. 62 (2010).
- [13] W. Haas, W. Rodi and B. Schonung, *The influence of density difference between hot and coolant gas on film cooling by a row of holes: Prediction and experiments*, ASME J. Turbo Machin. 114 (1992) 755–747.
- [14] J. Horlock, D. Watson and T. Jones, *Limitations on gas turbine performance imposed by large turbine cooling flows*, J. Eng. Gas Turb. Power 123(3) (2001) 494–487.
- [15] K.M. Kim, J.S. Park, D.H. Lee, T.W. Lee and H.H. Cho, *Analysis of conjugated heat transfer, stress and failure in a gas turbine blade with circular cooling passages*, Engin. Failure Anal. 18(4) (2011) 1212–1222.
- [16] C. Langowsky and D.T. Vogel, *Influence of film cooling on the secondary flow in a turbine nozzle*, AIAA 35(1) (1997).
- [17] S.-J. Li, J. Lee, J.-C. Han, L. Zhang and H.-K. Moon, *Influence of mainstream turbulence on turbine blade platform cooling from simulated swirl purge flow*, Appl. Thermal Eng. 101 (2016) 678–685.
- [18] Z. Liu and Z. Feng, *Numerical simulation on the effect of jet nozzle position on impingement cooling of gas turbine blade leading edge*, Int. J. Heat Mass Transfer 54(23–24) (2011) 4959–4949.
- [19] Y. Liu, L. Wang and Z.S. Qian, *Numerical investigation on the assistant restarting method of variable geometry for high Mach number inlet*, Aerosp. Sci. Technol. 79 (2018) 647–657.
- [20] Z. Liu, L. Ye, C. Wang and Z. Feng, *Numerical simulation on impingement and film composite cooling of blade leading edge model for gas turbine*, Appl. Thermal Eng. 73(2) (2014) 1432–1443.
- [21] W. MacCormack, O.R. Tutty and E. Rogers, *Stochastic optimization based control of boundary layer transition*, Control Engin. Practice 10 (2002) 260–243.
- [22] K. Mazaheri, M. Zeinalpour and H.R. Bokaei, *Turbine blade cooling passages optimization using reduced conjugate heat transfer methodology*, Appl. Thermal Eng. 103 (2016) 1228–1236.
- [23] A.B. Moskalenko and A.I. Kozhevnikova, *Estimation of gas turbine blades cooling efficiency*, Int. Conf. Industrial Engin. ICIE, (2016).
- [24] R. Roy, A. Tiwari and J. Corbett, *Designing a turbine blades cooling system using a generalize regression genetic algorithm*, CIRP Ann. 52(1) (2003) 415–418.
- [25] H. Sun, S. Bu, Y. Luan, T. Sun and X. Pei, *Numerical research on the film cooling gas turbine blade with the conjugate heat transfer method*, Materials Res. Innov. 19(6) (2015) 180–175.
- [26] L. Torbidoni and A.F. Massardo, *Analytical blade row cooling model for innovative gas turbine cycle evaluations supported by semi-empirical air cooled blade data*, Proc. ASME Turbo Expo Amsterdam, Netherlands, (2002).
- [27] K. Yu, J. Xu, Z. Lv and G. Song, *Inverse design methodology on a single expansion ramp nozzle for scramjets*, Aerosp. Sci. Technol. 92 (2019) 9–19.